
Article:
Glover, ZJ, Francis, MJ orcid.org/0000-0002-7033-7368, Fiutowski, J et al. (7 more authors) (2020) Acoustic attenuation spectroscopy and helium ion microscopy study of rehydration of dairy powder. Colloids and Surfaces A: Physicochemical and Engineering Aspects, 600. 124795. ISSN 0927-7757

https://doi.org/10.1016/j.colsurfa.2020.124795

Acoustic attenuation spectroscopy and helium ion microscopy study of rehydration of dairy powder

Zachary J. Glover[a,b,*], Mathew J. Francis[b], Jacek Fiutowski[c], Qinxin Sun[b], Qinya Yu[b], Ulf Andersen[d], Jonathan R. Brewer[e], Adam Cohen Simonsen[a], Megan J. Povey[b], Melvin J. Holmes[b]

[a]*Department of Physics, Chemistry and Pharmacy, University of Southern Denmark,Campusvej 55,5230 Odense, Denmark*
[b]*School of Food Science and Nutrition, University of Leeds,LS2 9JT, UK*
[c]*Mads Clausen Institut, NanoSYD, University of Southern Denmark, Alsion 2, 6400 Sønderborg, Denmark*
[d]*Arla Foods a.m.b.a, Agro Food Park 19, 8200 Aarhus, Denmark*
[e]*Department of Biochemistry and Molecular Biology,University of Southern Denmark,Campusvej 55,5230 Odense, Denmark*

Abstract

Complete hydration is essential for the production of structured dairy products from powders. It is essential that the ingredients used hydrate completely. Determination of an end point of rehydration is non-trivial, but ultrasound-based methodologies have demonstrated potential in this area and are well suited to measuring bulk samples in-situ. Here, Acoustic Attenuation Spectroscopy (AAS) is used to monitor rehydration of skim milk powder, and recombined systems of micellar casein isolate (MCI) with lactose and whey protein isolate (WPI). Dynamic light scattering, zeta-potential measurements and AAS as a function of pH characterise each component around its isoelectric point to assess its functionality. Scanning helium ion

*Corresponding author
Email address: glover@sdu.dk (Zachary J. Glover)

microscopy was used to image the dry powders, without any conductive coating, producing resolution equivalent to Scanning Electron Microscopy, but with much larger focal lengths and fewer imaging artefacts. Imaging the powders provides information on particle size and morphology which can affect dissolution behaviour. Reconstituted skim milk powder and recombined samples were monitored showing there are changes occurring over several hours. Attenuation coefficients are shown to predict the end point of hydration. Model fitting is used to extract volume fractions and average particle sizes of large and small particle populations in recombined samples over time. AAS is demonstrated to be capable of tracking the dynamics in rehydrating dispersions over time. Physical parameters such as the volume fraction and particle size of the dispersed phase can be determined.

Keywords: Acoustic Attenuation Spectroscopy, Ultrasound spectroscopy, Scanning Helium Ion Microscopy, Powder Rehydration, ECAH Model

---

1. Introduction

Globally, there is a big advantage to shipping food in the form of powders which have much lower volume than their fresh counterparts, have extended shelf lives due to low water activity, can be stored under ambient condition and then reconstituted at the location where they will be consumed or further processed [1, 2]. The manufacture and shipping of dairy derived powders allows the dairy industry to access new markets. Improvements in the dairy industry in fractionation technologies and in extracting individual components from side streams, such as whey from cheese making, has provided the potential for novel, high-value and easily handled powdered ingredients [3–5].

One current challenge is the ability to either completely reconstitute a single powder, or to rehydrate a blend of multiple powders to create a recombined product and ensure that the functionality of the system is equivalent to the fresh system from which it is derived [6, 7]. Through the drying and subsequent reconstitution process changes in the functionality of dairy systems occur that affect structural and rheological properties of the final dairy gels [8–10]. Methods are required to characterise the rehydration of individual and recombined systems to better understand when hydration has been achieved, or when the system is in optimal condition for product manufacture. Acoustic Attenuation Spectroscopy (AAS) has been demonstrated to be effective in monitoring aggregation in micellar casein isolate (MCI) dispersions [11].

When reconstituting powders there is a complex interplay between the powder(s) and solvent. In model systems studied at a lab scale there are several stages of powder dissolution, where the powder must first be wet-

ted by the liquid, the powder particles then sink, sediment and swell before the powder particles disintegrate [12–14]. Industrially reconstitution is conducted under more aggressive mixing regimes, however understandings based on model systems can be scaled up to further optimise the industrial process. It has been noted that surface composition plays a significant role in powder wettability [12]. Dispersability is affected by the protein content, specifically casein [15, 16] where the formation of an insoluble interfacial surface around the particle can reduce its ability to break down [17, 18]. Following dissolution, the reconstituted system may appear to be similar to the native system, but the solubilised or dispersed individual components that have been may require a longer period of time to fully hydrate and establish an equilibrium [19–26].

In skim milk the major components, other than water, by mass are the disaccharide lactose (5 %), and protein (4 %, 80 % of which are caseins) and the remainder is the water-soluble whey protein fraction [10]. Caseins are present in the form of casein micelles which are roughly spherical structures in which well hydrated, individual casein molecules are held together through hydrophobic interactions, hydrogen bonding and ionic interactions between phospho-serine residues and the presence of calcium phosphate nano-clusters [27–29]. Calcium, therefore, plays an integral structural role in the casein micelles, and shifting ionic equilibria between the free ionic calcium, calcium bound to protein and calcium in the form of calcium phosphate nano-clusters will affect the structure and functionality of the casein micelles [30, 31]. Different processing methods lead to the production of powders that have distinct physical properties including size distribution, powder morphology,

power packing, flowability and wettability [16].

Understanding the physical properties of the powder, such as its particle size distribution, can aid in understanding the wetting and dissolution behaviour of the powder. Scanning Electron Microscopy (SEM) has been widely used to image powder particles, which can require a conductive coating to be applied to the sample surface [14, 16] with subsequent problems of artefacts. Scanning Helium Ion Microscopy (HIM) provides an alternative to SEM, with the same nanometer resolution and a longer focal length, but without requiring any conductive coating. HIM offers a method to image native powder rapidly, ensuring there is no loss of surface information from the application of a conductive sample coating. Helium ion microscopy has great potential within food science, with the ability to accurately probe a materials surface and adjacent interiors. Different ion beams can be allow the sample to be physically etched revealing 3D information about the samples structure [32–35]. HIM has so far not been fully exploited in the imaging of food structures, particularly samples that are already in a dry state.

Ultrasound based measurements are well suited to monitoring rapidly changing complex colloidal systems such as, protein aggregation [11] or the enzymatic degradation of gels [36]. Acoustic analysis techniques can measure concentrated systems, without dilution and can be used for on-line monitoring during production [37]. Velocimetry measurements provide information on dynamic changes in a system, such as powder dissolution, with results comparable to other measurement techniques [11, 38]. AAS involves measures the absolute acoustic attenuation as a function of frequency over a broad range of frequencies (1-120 MHz) and can measure emulsions with vol-

ume fractions from 0.5 to 50 %, dependent upon physical properties, and may predict particle sizes in the range 0.01 μm to 1000 μm [39, 40]. AAS has been used previously to assess the degree of denaturation in bovine serum albumin [41], characterise oil-in-water emulsions [42], reconstituted milk powder [43] and particle sizing in dairy beverages [19]. This research suggests that AAS is an excellent technique for monitoring changes (particularly slower changes taking place over many hours) in rehydrating recombined systems comprised of multiple dairy derived ingredients.

A toolkit for the better understanding of the effects of temperature, time, pH, shear forces, solvent quality, mineral balance and buffering capacity and the ability to determine an effective end point of rehydration would improve process optimisation. Powders produced under different conditions have altered compositions and functionalities to their native equivalents. Previously, alternative technologies have been utilised to monitor powder dissolution and powder solubility, including; using static light scattering (SLS) [14], with a focussed beam reflectance measurement (FBRM) [38], Dynamic light scattering (DLS), turbidity measurements with transmission electron microscopy (TEM) [44], and optical image analysis to monitor particle size [25], contact angle measurements, particle sizing and sedimentation [45], solubility tests with gel electrophoresis and mass spectrometry [17]. An advantage of the acoustic techniques is that they can be applied on-line and non-invasively to monitor rehydration in food processes without requiring sampling and off-line analysis.

In this paper four powders - skim milk powder (SMP), micellar casein isolate (MCI), whey protein isolate (WPI) and lactose (see table 1) have been

imaged with HIM which is capable of discerning differences in the powder particle morphologies whereby a better understanding of wetting and dissolution can be obtained. Acoustic attenuation spectroscopy is used to track changes in recombined dairy samples over time as the samples hydrate. We show that AAS is capable of detecting changes in rehydrating skim milk powder, occurring on the order of 8 hours. SMP, lactose and WPI dispersions are characterised acoustically, with DLS based particle size and zeta potential measurements. Casein has been identified as the component responsible for poor solubility and rehydration, selected MCI samples were recombined with lactose, WPI or both lactose and WPI [13, 17, 22]. AAS measurements can be inverted to yield particle size and volume information of the dispersed phases. Changes in acoustic spectra and predicted particle sizes and volume fractions support the observation that over time larger particles continue to break up into smaller particles which are hydrating.

2. Materials & Methods

2.1. Scanning Helium Ion Microscopy

An ORION NanoFab Helium Ion Microscope (Zeiss, Oberkochen, Germany) was used to image the four dairy derived powders under investigation, equipped with Secondary Electron detection and operated at 25 keV beam energy with a probe current ranging from 0.15 to 0.25 pA. The samples were prepared for imaging by distributing small quantities of powder onto carbon tape that was fixed to an aluminium sample plate (Plano GmbH, Wetzlar, Germany). No conductive coatings were applied to the samples prior to imaging to preserve sample surface information. Charge compensation was

ensured through a low-energy electron beam using a flood gun, 600 eV.

2.2. Sample preparation

All reconstituted powder samples were mixed using a magnetic stirrer set to create turbulent mixing conditions whilst minimising vortexing to reduce aeration. Powders were added to liquid gradually before either having the pH adjusted and/or being transferred to the measurement devices and monitored over time. Powder compositions given by the manufacturer are shown in table 1.

	Protein (%)	Fat (%)	Lactose (%)	Ash (%)
SMP	34	1.25	54	8
MCI	86	1.5	4	8
WPI	92	0.2	0.2	4.5
Lactose	0.2	-	99	0.3

Table 1: Composition of the dairy derived powders used in this study as given by the manufacturer on a dry matter basis

Fresh skim milk used was locally purchased (Arla Foods a.m.b.a., UK.). 10 % (w/w) reconstituted medium heat skim milk powder (SMP) (Arla Foods, a.m.b.a, Denmark) samples were prepared by adding SMP to MilliQ water (Millipore, Bedford, UK). The mineral content from the fresh milk is preserved in SMP so other ions were not added in for this sample.

Powder samples were all industrially pray dried without an agglomeration processing step. Samples of micellar casein isolate (MCI) (Ingredia Functional, Arras, France), whey protein isolate (WPI)(Arla Foods, a.m.b.a, Denmark) and lactose (Arla Foods, a.m.b.a, Denmark), and combination of

the above were prepared with solutions of 0.1 M NaOH (Fluka, USA) to maintain consistency with sample preparations utilised previously [11]. The final pH of the solutions were then adjusted using either 1 M hydrochloric acid (Fluka, USA) and/or 1 M sodium hydroxide (Fluka, USA) when required. The samples prepared and used in this study are shown in table 2. In line with previous work [11] 0.8 % MCI powder was used which gave a hydrated volume fraction (4 %) that could be accurately fitted with the ECAH model used on the acoustic data. Quantities of lactose and WPI were kept as close to the values occurring in fresh skim milk as possible.

Sample	Conc (w/w)	Against	Equipment
SMP	10 %	pH (3.5-5.5)	U + Z
		time (pH 6.54)	U
Lactose	5 %	pH (3.5-5.5)	U + Z
WPI	0.8 %	pH (4-6)	U + Z
MCI + Lactose	0.8 + 5 %	time (pH 6.7)	U
MCI + WPI	0.8 + 0.8 %	time(pH 6.7)	U
MCI + Lactose + WPI	0.8 + 5 + 0.8 %	time (pH 6.7)	U
Fresh skim milk	-	-	U

Table 2: Reconstituted and recombined dairy derived samples under investigation. Details include the type of powder used, concentration, whether investigated over a pH range or time and whether assessed with the acoustic based Ultrasizer (U), or light based Zetasizer (Z).

The pH of the different dispersions and solutions was adjusted using a potentiometric titrator (pH Stat) (Metrohm, Switzerland). The potentiometric titrator used consisted of a 902 Titrando unit and an 801 stirrer. The pH

was controlled to within 0.001 pH unit using the Tiamo software. The pH of the samples were adjusted in steps of 0.5 pH units using the pH Stat for both light based and acoustic based measurements. Samples were repeated in triplicate (n=3) and kept at 25 °C throughout titration and subsequent measurements. The WPI solution was measured over a higher pH range due to its higher isoelectric point.

2.3. Zeta-potential and Dynamic Light Scattering Measurements

The zeta potential and particle size distribution of reconstituted dairy systems was determined at different pH values using a Zetasizer Nano ZS (Malvern Pananalytical, UK). Measurements were made at 25 °C, using 1-2 drops of sample per cuvette diluted with MiliQ water up to approximately 2 ml for zeta potential measurements and particle measurements which were conducted separately.

2.4. Acoustic Attenuation Spectra

An Ultrasizer MSV (Malvern Instruments, UK) was used to measure the attenuation spectrum of the different reconstituted and recombined dairy dispersions, either at different pH values, or monitoring the change in spectra over time at pH 6.7, the pH of native bovine milk. The Malvern Ultrasizer MSV produces acoustic spectra in the range 1 – 120 MHz with precision ±1 dB / 0.115 Np. Convergence in the higher frequency data will be more apparent on a log-scale plot as the error will be minimised. 500 ml of sample is required for the Ultrasizer measurements. The temperature was set and kept at 25 °C by an external temperature control unit (Huber Ministat, Germany). An overhead stirrer was set at 400 rpm to limit thermal gradients

within the sample. Measurement options were set as 50 frequency points, 30 measurements per frequency, 10 repeat measurements.

The attenuation coefficient, α (Npm^{-1}) is dependent on frequency and can be determined by fitting equation 1 to the attenuation spectrum showing attenuation as a function of frequency,

$$\alpha = Af^n \tag{1}$$

A is a pre-factor which is dependent upon physical parameters (see equation 4) and f, (MHz) is the frequency. For Newtonian fluids the exponent n takes the value of 2 but varies with other fluids and emulsions and is affected by molecular relaxation effects [39].

2.5. Data inversion to Particle Size and Volume Fraction

In order to be able to quantitatively describe the rehydrating systems, data inversion from the AAS is required. The attenuation spectra obtained from the Ultrasizer can be inverted using scattering theory, the so called ECAH model (Epstein Carhart, Allegra and Hawley), [46, 47] to produce particle size and volume fraction of a dispersed phase in reconstituted dairy systems [11]. The attenuation of an acoustic wave having angular frequency ω decays exponentially with distance where wave amplitude $A(x,t)$ at spatial point x from the origin at time, t is given by equation 2

$$A(x,t) = A_0 e^{i(\omega t - k_C\ x)} \tag{2}$$

where i is the imaginary number equal to $\sqrt{-1}$, and k_C is the complex compressional wavenumber (equation 4).

198 The ECAH model predicts the attenuation α $[Npm^{-1}$ or $dBm^{-1}]$ due to
199 a particle of a known radius r and volume fraction ϕ at each frequency f
200 (MHz) of the incoming wave. Spherical harmonic solutions of the compres-
201 sional field, φ, consist of radial spherical Hankel functions h_n and Legendre
202 polynomials P_n and are shown in equation 3

$$\varphi = \sum_{n=0}^{\infty} i^n \left(2n+1\right) A_n h_n \left(k_C r\right) P_n \left(\cos\theta\right) \tag{3}$$

203 where k_C is the compressional wavenumber given in equation 4.

$$k_C = \frac{\omega}{\nu} + i\alpha = \frac{\omega}{\nu} + i\frac{\eta\omega^2}{2\rho\nu^3}\left[\frac{4}{3} + \frac{\mu}{\eta} + \frac{\left(\gamma-1\right)\tau}{\eta C_p}\right] \tag{4}$$

204 where ν is the velocity in the phase, ω the angular frequency, η is the shear
205 viscosity (Pas^{-1}), ρ is the density (kgm^{-3}), μ is the bulk viscosity (Pas^{-1}), γ
206 is the ratio of specific heats, τ is the thermal conductivity $(Wm^{-1}K^{-1})$, C_p is
207 the specific heat at constant pressure $(Jkg^{-1}K^{-1})$ and A_n are the scattering
208 coefficients determined from solution of the boundary value problem [39,
209 40, 48–51]. The physical properties of the dispersed phase used in these
210 calculations are given in table 3.

211 The scattering contribution attributed to the ensemble of particles is
212 characterised by the excess attenuation, shown in equation 5 determined
213 by subtracting the attenuation from the pure continuous phase and from the
214 dispersed droplets in proportion to their associated volume fractions,

$$\alpha_{excess} = \alpha_{total} - (1-\phi)\alpha_{continuous} - \phi\,\alpha_{dispersed} \tag{5}$$

215 Experimentally, measured attenuation spectra at each frequency f_i (i =

	Water	Casein
Ultrasound velocity (ms^{-1})	1497	1563
Density (kgm^{-3})	997	1076
Specific heat capacity ($Jkg^{-1}K^{-1}$)	4177	3818
Thermal conductivity ($Wm^{-1}K^{-1}$)	0.611	0.521
Thermal expansivity (K^{-1})	2.1 x 10^{-4}	7.5 x 10^{-4}
Attenuation exponent (MHz^{-2})	2.0	1.4
Attenuation coefficient (Np m^{-1})	0.023	4.02

Table 3: Physical properties of water and casein at 25 °C used in the numerical calculation to solve the ECAH model from the attenuation spectra [39, 51–53]

1,. . . ,n frequencies) are evaluated and minimised against model predictions e.g. using a sum-squared residual fit (SSD) as in equation 6 [43].

$$SSD = \sum_{i=1}^{n} [\alpha_T(f_i) - \alpha_E(f_i)]^2 \tag{6}$$

where T is theoretical and E is experimental, thus providing particle size and volume fraction estimates of the particle size and volume fraction distributions.

3. Results & Discussion

3.1. Scanning Helium Ion Microscopy of Dairy Powders

Scanning helium ion microcopy was used to image the four dairy derived powders under investigation as can be seen in figure 1. Note that the powders show differences in particle size and in morphology. SMP (1a-b) has spherical particles that all exhibited a pleated surface structure. Comparatively the WPI (1c-d) and MCI (1e-f) have smooth surfaces. The WPI has spherical structures, whereas the MCI shows more irregular structures. The lactose (1g-h) powder has much more irregular particles, including regions that appear crystalline in nature and overall finer surface structures than is seen in the other three powders. As no sample preparation or coating is required with helium ion microscopy the differences in powder surface morphology that can be observed in figure 1 cannot have been obscured or modified by addition of a coating. When powders are added to water initial wetting of the particles is important and it has been shown that in general larger particles are more wettable, contributed to by the smaller surface area to volume ratio. Powder sample images can show the degree to which the particles are agglomerated, which facilitates wetting by reducing the effective surface area to volume ratio, and providing multiple channels for water to penetrate through which is aided by capillary forces. Gaiani et al., [15] noted that agglomeration improved the wetting of whey based powders but casein based powders performed better without agglomeration. The images in figure 1 show that the WPI particles have some degree of agglomeration, which is likely to improve its dissolution. The MCI powder has less agglomeration, although there are a number of small particles observable together with the

larger particles, the large surface area to volume ratio of such small particles could have contributed to the slow hydration rate observed with the MCI (figure 5). The ability to quickly image powders can provide feedback on the degree of agglomeration, and therefore provide insights into how it may perform, especially when it can be compared to information on rehydration over time. Helium ion microscopy could provide an invaluable tool to the powder scientist when comparing the effects of different formulations in optimising a drying process, allowing the native particles to be imaged quickly.

3.2. Rehydration of Skim Milk Powder

The acoustic attenuation spectrum was monitored for 10 % reconstituted skim milk powder dispersions, from which the attenuation coefficients were determined and compared to those of fresh skim milk, as shown in figure 2. It can be seen in figure 2a that the attenuation spectra changes over time, with convergence at higher frequencies. The attenuation decreases with increased hydration time at lower frequencies, which is clear in the raw attenuation spectrum. A projected end point has been determined by comparing two components of the attenuation coefficient from the rehydrating system to fresh skim milk. Extrapolating the pre-factor, A (figure 2b), with an exponential fit gives an end point of 7.5 hours, whilst extrapolating the exponent, n (figure 2c), with a linear fit gives an end point of 9.43 hours, where the attenuation would match that of fresh skim milk, these rehydration time are in agreement with previous studies on MCI [23] and MPC [14] powders. The pre-factor of the attenuation coefficient are affected by several physical parameters which can be seen in equation 4 including the shear η and bulk μ viscosities, the density ρ, the ratio of specific heats γ, the thermal conductiv-

ity τ, and the specific heat C_p, changes in these physical properties are therefore reflected in the pre-factor of the attenuation coefficient. The exponent is not directly related to any precise physical parameters but is affected by molecular relaxation effects, for Newtonian solutions the angular frequency ω has an exponent of 2. The exponent deviates in dispersions which exhibit scattering contributions, meaning that changes in the exponent value can be used to track changes in the physical behaviour of the system. Monitoring the attenuation spectra of a rehydrating skim milk powder dispersion over time allows the detection of changes occurring on a long time-scale, which were not detected with light scattering or simple acoustic velocimetry in preliminary experimentation (data not shown). Slow changes are likely to relate to the complete release of casein particles from the primary powder particles [14] and the equilibration of the mineral content in the sample, where the pH and colloidal calcium content have been shown to equilibrate slowly [54]. Having demonstrated that AAS is capable of detecting long order changes in rehydrating systems, it was then of interest to use this technique to investigate the influence of the individual macro-components present in the skim milk powder, and how they influence each other during rehydration.

The kinetics of dissolution would be of interest in different powders with varying composition, but for this study individual components were introduced as separate powders, recombined and then monitored as a function of pH and/or time. The properties of micellar casein isolate solutions were previously characterised acoustically [11], including zeta potential and DLS particle sizing. Three separate powders were used in isolation and combination to better understand whether the effects of different components on the

rehydration of recombined systems can be detected acoustically.

3.3. Zeta Potential and PSD of Dairy Systems as a function of pH

The zeta potential and mean particle size, given as the diameter of a sphere with equivalent volume to the particle of interest (D[3,2]), for reconstituted dispersions of SMP and WPI are shown in figure 3. The lactose under investigation forms a solution and so was not assessed by zeta-potential or DLS. The MCI under investigation has previously been characterised in the same manner as the SMP and WPI have been in this study [11]. Figure 3a shows that the isoelectric point of the reconstituted SMP is between 4.0-4.5 and approximately 4.25, which is below the native pI casein, 4.6. The previously recorded pI for reconstituted MCI was between pH 4.3 -4.7 [11] which is closer to the native pI of casein. Figure 3c shows that the isoelectric point of the WPI is higher than that of the SMP and MCI values, between 4.5-5.0, approximately 4.75. The isoelectric point of whey protein, 5.2 for β-lactoglobulin, is higher than that of the caseins and so WPI would be expected to have a higher pI [55]. The mean particle size as a function of pH for SMP shows a slight trend towards peaking around the determined pI, although the trend is weak in comparison to variation seen, so there is no clear evidence of aggregation occurring. Rapid changes in pH are more likely to lead to precipitation of the caseins in a skim milk dispersion, rather than aggregation and network formation, which is more likely to occur when titrating with a strong acidic solution. The mean particle size of the WPI dispersions as a function of pH is very variable, suggesting that at different surface charges there are more complex intermolecular interactions occurring, which facilitate small particle sizes at pH values of 4.5 and 6.0, and larger

aggregated states at pH values of 4.0, 5.0 and 5.5. The aggregation state of β-lactoglobulin has been well characterised and is affected by pH, salt concentration and temperature [56–58], the WPI contains other whey proteins too, which is likely why the aggregation behaviour with pH is complex. Further work would be required to unpick the mechanisms of aggregation that have been observed in the DLS data. The variable particle size information shown in figure 3d may be in part due to using small sample volumes and the presence of larger protein aggregates, which highlights the benefit of using a bulk method such as AAS. Following assessment with the zeta-sizer and varying pH the same samples could be evaluated with AAS and compared to results obtained from a light based method, the Ultrasizer is capable of making particle size measurements in the range where aggregation occurs.

3.4. Attenuation Spectra of Dairy Systems as function of pH

The acoustic attenuation spectra of reconstituted SMP, WPI and lactose are shown in figure 4. From figure 4a it can be seen that AAS for WPI dispersions as function of pH is broadly similar over the majority of the frequency range. At the lowest frequencies the curves diverge from one another slightly, with decreasing attenuation from pH $4.5 > 5.0$. $4.0 > 5.5 > 6.0$, which with the exception of the pH 6.0 data follows the trend in the mean particle size shown in figure 3b. At increased particle size there is a decrease in the attenuation which would be expected given that small particles in acoustic fields scatter more than large particles, the reverse of optical scattering [39]. The AAS of reconstituted SMP dispersions as a function of pH shows increased scattering at the pI across the low frequency range, as seen in figure 4b. Increased scattering at the isoelectric point suggests that particle

aggregation has occured. Aggregation may have been more likely to occur in the Ultrasizer which has a large volume under constant agitation, which may promote inter-particle aggregation compared to the samples measure in a cuvette in the Zetasizer, where less change was observed at the isoelectric. The AAS of lactose solutions as a function of pH do not show any trends, as would be expected of a sugar solution, as seen in figure 4. As has been previously demonstrated with MCI dispersions the Ultrasizer is capable of detecting aggregation of protein in the region of the isoelectric point for casein based systems, and shows a slight trend between DLS based particle size and acoustic attenuation at low frequency for whey protein isolate dispersions. Micellar casein is likely to be a stronger scatterer than the water soluble whey proteins, which is why the changes in AAS are greater for the casein containing systems. Having characterised the individual components as a function of pH, and shown that AAS is capable of detection aggregation of proteinaceous particles, the hydration of the samples was investigated over time.

3.5. Attenuation Spectra of Recombined Dairy Systems Over Time

Micellar casein has been shown to be a strongly scattering species in reconstituted dairy systems of MCI ([11] and SMP (figure 4). Micellar casein is the component responsible for the majority of structure formation in many fermented dairy products and therefore it is the component of primary interest in this study to better monitor the rehydration of recombined dairy systems. Select composite samples have been chosen to evaluate the capability of AAS in differentiating the rehydration behaviour of different dairy systems, when multiple components have been mixed together and left to

reach an equilibrium state. Providing that AAS is capable of differentiating distinct sample behaviour it can then be used in future systematic studies of the effects of other compositional elements such as the calcium content, overall mineral balance and ratios of macro components.

MCI has been investigated in different recombined systems of MCI with lactose, MCI with WPI and MCI with lactose and WPI. The recombined systems have been monitored over time to establish whether the presence of other macro components in the recombined dispersion increase the rate at which the system finds an equilibrium, or no further changes can be detected. Figures 5a & b compare the effects of recombining the MCI with 5 % lactose (b) or 0.8 % WPI (c) and then monitoring the AAS over time. The system that includes lactose reaches an end point much sooner than the solution without lactose. Comparatively the MCI + WPI system shows a trend similar to the SMP shown in figure 2a, where there is a clear decrease in the attenuation at lower frequencies with time, whilst there is convergence at higher frequencies, with the system reaching stability after 90 minutes. Whilst it is known that powders containing more soluble components such as whey and minerals increase the rate of powder dissolution [15], it has been shown that having lactose present in a recombined system aids the rehydration of the MCI as well, even though not present in the actual powder during the dissolution stage. It has been shown there is no significant difference in rehydration between dry-mixing or co-drying casein with lactose or ultrafiltrate [22], where the soluble components prevent sticking of the dispersing protein particles. Dry mixing proteins after spray drying has been shown to lead to longer rehydration times [**?**]. Dry-blending has shown improvements

in dairy powder solubility for mineral addition [59] and sodium caseinate addition [60]. A recombined sample containing MCI, WPI and lactose was evaluated over time using AAS the data from which is shown in figure 5c. Figure 5c shows the raw attenuation spectra over time, from which is can be seen that there is clear trend with increasing rehydration time. The total time represented in figure 5c is 12 hours, the figure shows convergence at higher frequencies, but clear changes in the low frequency data, as in the case for the reconstituted SMP in figure 2a and the MCI + WPI in figure 5b. As the same trends are observed in figures 2a and 5c, it can be noted that the main behaviour of the rehydrating SMP is captured in the reconstituted sample, any offset will be due to compositional differences in mineral balance and exact ratios of macroscopic components. Furthermore, monitoring the attenuation coefficients as they tend towards a reference point would be a suitable method of predicting an end point . As the powders rehydrate there will be changes in the overall physical properties of the system, which are captured within the compressional wavenumber equation 4.

3.6. Data Inversion of Rehydrating Dairy System

The excess attenuation is calculated using equation 5 and then expressed as the product of attenuation and wavelength $\alpha\lambda$. The experimentally measured AAS is evaluated against model predications using a sum-squared residual fit shown in equation 6. Optimum particle size and volume fractions are determined by random sampling and searching the parameter space. Fitting relies on initial estimates of the particle size but a suitable range is applied to ensure all reasonable sizes are explored. The volume fraction initial estimate is already known but this is optimised and therefore ensures the predictions

agree with expected volumes. As can be seen in figure 6 for fresh skim milk, the whole spectrum is not fitted by a single component, however, a better fit can be achieved when a large particle fit, for lower frequencies and a small particle fit for higher frequencies are used. The same physical properties are used for both the large and small particle fits as the physical composition of these two populations is expected to be the same. The large and small particle component fits can be added to produce a combined fit, which better represents the experimental data. A linear superposition of the small and large particle model fits is achieved by again applying a minimisation of a residual fit. Model fitting can then be applied to experimental data sets to quantify how the volume fraction and particle size of different population of particle change over time as shown in table 4.

	ϕ_{small} (%)	r_{small} (nm)	ϕ_{large} (%)	r_{large} (nm)
Fresh skim milk	3.32	36	1.75	126
Recombined 0.5h	0.73	56	4.61	938
Recombined 3h	1.01	54	1.27	1145
Recombined 6h	0.93	55	1.44	1207
Recombined 12h	1.01	52	1.46	1182

Table 4: Volume fraction and particle size predictions extracted from attenuation spectra using the ECAH model for fresh skim milk and recombined MCI + WPI + lactose with increased hydration time.

Figure 5c shows data over a 12 hour period, select time points at 0.5, 3, 6 and 12 hours have been inverted using the ECAH model to provide volume fraction and particle size information, compared to fresh skim milk. The fitted data is shown in figure 7 for the recombined sample and fresh milk,

the inverted data is shown in table 4. The fitted data shows that there is a trend in the rehydrating sample that initially has a large particle population with a large volume fraction, which decreases in volume fraction over time, meaning there are less larger particles in the system. Over time the large particle population increases in size suggesting swelling due to hydration over time. The small particle population does not change in size, however there is an initial increase in the volume fraction of the small particle population from 0.5- 3 hours, indicating that the larger particle population is breaking down into smaller particles. The data presented here shows that it is possible to track the rehydration behaviour of different dairy derived powders, when in combination with each other. Data inversion of the AAS using the ECAH model can provide relevant quantification, and provide physical parameters upon which conclusions about the system can be drawn.

4. Conclusions

Overall it has been demonstrated that AAS can be utilised to track the rehydration processes that occur in recombined and reconstituted systems. Scanning HIM has been used to image dry powder particles without coating to reveal surface details and show the degree of powder agglomeration, information that can be used to understand the wetting behaviour of a powder. There are slow changes that take place well beyond the process of powder dissolution, which can be detected with AAS. AAS is capable of characterising individual components as a function of pH and time, being sensitive to both temporal changes in the dispersed phase and aggregation phenomena. AAS is sensitive enough to respond to the presence of individual components,

not just to the behaviour of the dominant scattering species present. Data inversion with the ECAH model allows quantification of the particle size and volume fraction of the dispersed phase, providing meaningful physical parameters about the system.

Acknowledgements

This work was funded by Arla Foods a.m.b.a., Denmark.

Competing interest statement

The authors have no competing interests.

References

[1] V. Lagrange, D. Whitsett, C. Burris, Global market for dairy proteins, Journal of food science 80 (S1) (2015) A16–A22.

[2] P. M. Kelly, Innovation in milk powder technology, International journal of dairy technology 59 (2) (2006) 70–75.

[3] G. Brans, C. Schroën, R. Van der Sman, R. Boom, Membrane fractionation of milk: state of the art and challenges, Journal of Membrane Science 243 (1-2) (2004) 263–272.

[4] Y. Pouliot, Membrane processes in dairy technology—from a simple idea to worldwide panacea, International Dairy Journal 18 (7) (2008) 735–740.

[5] A. Saxena, B. P. Tripathi, M. Kumar, V. K. Shahi, Membrane-based techniques for the separation and purification of proteins: An overview, Advances in colloid and interface science 145 (1-2) (2009) 1–22.

[6] G. S. Meena, A. K. Singh, N. R. Panjagari, S. Arora, Milk protein concentrates: opportunities and challenges, Journal of food science and technology 54 (10) (2017) 3010–3024.

[7] Y. Lin, A. L. Kelly, J. A. O'Mahony, T. P. Guinee, Effect of heat treatment, evaporation and spray drying during skim milk powder manufacture on the compositional and processing characteristics of reconstituted skim milk and concentrate, International Dairy Journal 78 (2018) 53–64.

[8] Z. J. Glover, C. Ersch, U. Andersen, M. J. Holmes, M. J. Povey, J. R. Brewer, A. C. Simonsen, Super-resolution microscopy and empirically validated autocorrelation image analysis discriminates microstructures of dairy derived gels, Food hydrocolloids 90 (2019) 62–71.

[9] Z. J. Glover, M. J. Francis, A. H. Bisgaard, U. Andersen, L. B. Johansen, M. J. Povey, M. J. Holmes, J. R. Brewer, A. C. Simonsen, Dynamic moisture loss explored through quantitative super-resolution microscopy, spatial micro-viscosity and macroscopic analyses in acid milk gels, Food Hydrocolloids 101 (2020) 105501.

[10] H. Eshpari, R. Jimenez-Flores, P. Tong, M. Corredig, Partial calcium depletion during membrane filtration affects gelation of reconstituted milk protein concentrates, Journal of dairy science 98 (12) (2015) 8454–8463.

[11] M. Francis, Z. Glover, Q. Yu, M. Povey, M. Holmes, Acoustic characterisation of ph dependant reversible micellar casein aggregation, Colloids and Surfaces A: Physicochemical and Engineering Aspects 568 (2019) 259–265.

[12] E. H.-J. Kim, X. D. Chen, D. Pearce, Surface characterization of four industrial spray-dried dairy powders in relation to chemical composition, structure and wetting property, Colloids and surfaces B: Biointerfaces 26 (3) (2002) 197–212.

[13] Y. Fang, C. Selomulya, S. Ainsworth, M. Palmer, X. D. Chen, On quantifying the dissolution behaviour of milk protein concentrate, Food Hydrocolloids 25 (3) (2011) 503–510.

[14] A. Mimouni, H. C. Deeth, A. K. Whittaker, M. J. Gidley, B. R. Bhandari, Rehydration process of milk protein concentrate powder monitored by static light scattering, Food Hydrocolloids 23 (7) (2009) 1958–1965.

[15] C. Gaiani, M. Morand, C. Sanchez, E. A. Tehrany, M. Jacquot, P. Schuck, R. Jeantet, J. Scher, How surface composition of high milk proteins powders is influenced by spray-drying temperature, Colloids and Surfaces B: Biointerfaces 75 (1) (2010) 377–384.

[16] J. V. Silva, J. A. O'Mahony, Flowability and wetting behaviour of milk protein ingredients as influenced by powder composition, particle size and microstructure, International Journal of Dairy Technology 70 (2) (2017) 277–286.

[17] S. Anema, D. Pinder, R. Hunter, Y. Hemar, Effects of storage temperature on the solubility of milk protein concentrate (mpc85), Food Hydrocolloids 20 (2-3) (2006) 386–393.

[18] I. Gazi, T. Huppertz, Influence of protein content and storage conditions on the solubility of caseins and whey proteins in milk protein concentrates, International dairy journal 46 (2015) 22–30.

[19] S. Meyer, S. Berrut, T. Goodenough, V. Rajendram, V. Pinfield, M. Povey, A comparative study of ultrasound and laser light diffraction techniques for particle size determination in dairy beverages, Measurement Science and Technology 17 (2) (2006) 289.

[20] Y. Fang, C. Selomulya, X. D. Chen, On measurement of food powder reconstitution properties, Drying technology 26 (1) (2007) 3–14.

[21] Y. Fang, C. Selomulya, X. D. Chen, Characterization of milk protein concentrate solubility using focused beam reflectance measurement, Dairy Science & Technology 90 (2-3) (2010) 253–270.

[22] C. Gaiani, S. Banon, J. Scher, P. Schuck, J. Hardy, Use of a turbidity sensor to characterize micellar casein powder rehydration: Influence of some technological effects, Journal of dairy Science 88 (8) (2005) 2700–2706.

[23] C. Gaiani, P. Schuck, J. Scher, S. Desobry, S. Banon, Dairy powder rehydration: influence of protein state, incorporation mode, and agglomeration, Journal of Dairy Science 90 (2) (2007) 570–581.

[24] R. Hussain, C. Gaiani, J. Scher, From high milk protein powders to the rehydrated dispersions in variable ionic environments: A review, Journal of food engineering 113 (3) (2012) 486–503.

[25] B. Richard, J.-F. Le Page, P. Schuck, C. André, R. Jeantet, G. Delaplace, Towards a better control of dairy powder rehydration processes, International Dairy Journal 31 (1) (2013) 18–28.

[26] R. Jeantet, P. Schuck, T. Six, C. Andre, G. Delaplace, The influence of stirring speed, temperature and solid concentration on the rehydration time of micellar casein powder, Dairy Science & Technology 90 (2-3) (2010) 225–236.

[27] J. A. Lucey, D. S. Horne, Perspectives on casein interactions, International Dairy Journal 85 (2018) 56–65.

[28] D. G. Dalgleish, M. Corredig, The structure of the casein micelle of milk and its changes during processing, Annual review of food science and technology 3 (2012) 449–467.

[29] C. De Kruif, Casein micelle interactions, International Dairy Journal 9 (3-6) (1999) 183–188.

[30] H. Eshpari, P. S. Tong, M. Corredig, Changes in particle size, calcium and phosphate solubilization, and microstructure of rehydrated milk protein concentrates, prepared from partially acidified milk, Dairy Science & Technology 96 (3) (2016) 329–343.

[31] E. de Kort, M. Minor, T. Snoeren, T. van Hooijdonk, E. van der Linden,

Effect of calcium chelators on physical changes in casein micelles in concentrated micellar casein solutions, International Dairy Journal 21 (12) (2011) 907–913.

[32] M. T. Postek, A. E. Vladár, Helium ion microscopy and its application to nanotechnology and nanometrology, Scanning: The Journal of Scanning Microscopies 30 (6) (2008) 457–462.

[33] N. P. Economou, J. A. Notte, W. B. Thompson, The history and development of the helium ion microscope, Scanning 34 (2) (2012) 83–89.

[34] S. M. Novikov, V. N. Popok, A. B. Evlyukhin, M. Hanif, P. Morgen, J. Fiutowski, J. Beermann, H.-G. Rubahn, S. I. Bozhevolnyi, Highly stable monocrystalline silver clusters for plasmonic applications, Langmuir 33 (24) (2017) 6062–6070.

[35] A. S. Terpstra, K. E. Shopsowitz, C. F. Gregory, A. P. Manning, C. A. Michal, W. Y. Hamad, J. Yang, M. J. MacLachlan, Helium ion microscopy: a new tool for imaging novel mesoporous silica and organosilica materials, Chemical Communications 49 (16) (2013) 1645–1647.

[36] M. Holmes, T. Southworth, N. Watson, M. Povey, Enzyme activity determination using ultrasound, in: Journal of Physics: Conference Series, Vol. 498, IOP Publishing, 2014, p. 012003.

[37] Y. Al-Aufi, B. Hewakandamby, G. Dimitrakis, M. Holmes, A. Hasan, N. Watson, Thin film thickness measurements in two phase annular flows using ultrasonic pulse echo techniques, Flow Measurement and Instrumentation 66 (2019) 67–78.

[38] M. Hauser, J. Amamcharla, Development of a method to characterize high-protein dairy powders using an ultrasonic flaw detector, Journal of dairy science 99 (2) (2016) 1056–1064.

[39] M. J. Povey, Ultrasonic Techniques for Fluids Characterization, Academic Press, 1997.

[40] M. J. Povey, Ultrasound particle sizing: A review, Particuology 11 (2) (2013) 135–147.

[41] M. J. Povey, J. D. Moore, J. Braybrook, H. Simons, R. Belchamber, M. Raganathan, V. Pinfield, Investigation of bovine serum albumin denaturation using ultrasonic spectroscopy, Food hydrocolloids 25 (5) (2011) 1233–1241.

[42] D. McClements, M. Povey, Scattering of ultrasound by emulsions, Journal of Physics D: Applied Physics 22 (1) (1989) 38.

[43] S. Meyer, V. S. Rajendram, M. J. Povey, Characterization of reconstituted milk powder by ultrasound spectroscopy, Journal of food quality 29 (4) (2006) 405–418.

[44] G. J. Martin, R. Williams, D. Dunstan, Comparison of casein micelles in raw and reconstituted skim milk, Journal of Dairy Science 90 (10) (2007) 4543–4551.

[45] S. V. Crowley, B. Desautel, I. Gazi, A. L. Kelly, T. Huppertz, J. A. O'Mahony, Rehydration characteristics of milk protein concentrate powders, Journal of Food Engineering 149 (2015) 105–113.

[46] P. S. Epstein, R. R. Carhart, The absorption of sound in suspensions and emulsions. i. water fog in air, The Journal of the Acoustical Society of America 25 (3) (1953) 553–565.

[47] J. Allegra, S. Hawley, Attenuation of sound in suspensions and emulsions: Theory and experiments, The Journal of the Acoustical Society of America 51 (5B) (1972) 1545–1564.

[48] P. Lloyd, M. Berry, Wave propagation through an assembly of spheres: Iv. relations between different multiple scattering theories, Proceedings of the Physical Society 91 (3) (1967) 678.

[49] M. J. Povey, Acoustic methods for particle characterisation, KONA Powder and Particle Journal 24 (2006) 126–133.

[50] R. Challis, M. Povey, M. Mather, A. Holmes, Ultrasound techniques for characterizing colloidal dispersions, Reports on progress in physics 68 (7) (2005) 1541.

[51] F. Alba, D. Higgs, R. Jack, P. Kippax, Ultrasound spectroscopy: A sound approach to sizing of concentrated particulates, Handbook on ultrasonic and dielectric characterization techniques for suspended particulates (1998).

[52] V. Del Grosso, C. Mader, Speed of sound in pure water, the Journal of the Acoustical Society of America 52 (5B) (1972) 1442–1446.

[53] S. Vance, J. M. Brown, Sound velocities and thermodynamic properties of water to 700 mpa and- 10 to 100

circ c, The Journal of the Acoustical Society of America 127 (1) (2010) 174–180.

[54] S. Anema, Y. Li, Re-equilibration of the minerals in skim milk during reconstitution, Milchwissenschaft 58 (3-4) (2003) 174–178.

[55] P. Walstra, J. T. Wouters, T. J. Geurts, Dairy science and technology, CRC press, 2005.

[56] H. McKenzie, W. Sawyer, Effect of ph on β-lactoglobulins, Nature 214 (5093) (1967) 1101–1104.

[57] M. Verheul, J. S. Pedersen, S. P. Roefs, K. G. de Kruif, Association behavior of native β-lactoglobulin, Biopolymers: Original Research on Biomolecules 49 (1) (1999) 11–20.

[58] M. Gottschalk, H. Nilsson, H. Roos, B. Halle, Protein self-association in solution: The bovine β-lactoglobulin dimer and octamer, Protein Science 12 (11) (2003) 2404–2411.

[59] P. Schuck, A. Davenel, F. Mariette, V. Briard, S. Mejean, M. Piot, Rehydration of casein powders: effects of added mineral salts and salt addition methods on water transfer, International Dairy Journal 12 (1) (2002) 51–57.

[60] F. Bot, S. V. Crowley, J. A. O'Mahony, Solubility enhancement of milk protein isolate by sodium caseinate addition: comparison between wet-and dry-blending approaches, International Dairy Journal (2020) 104661.

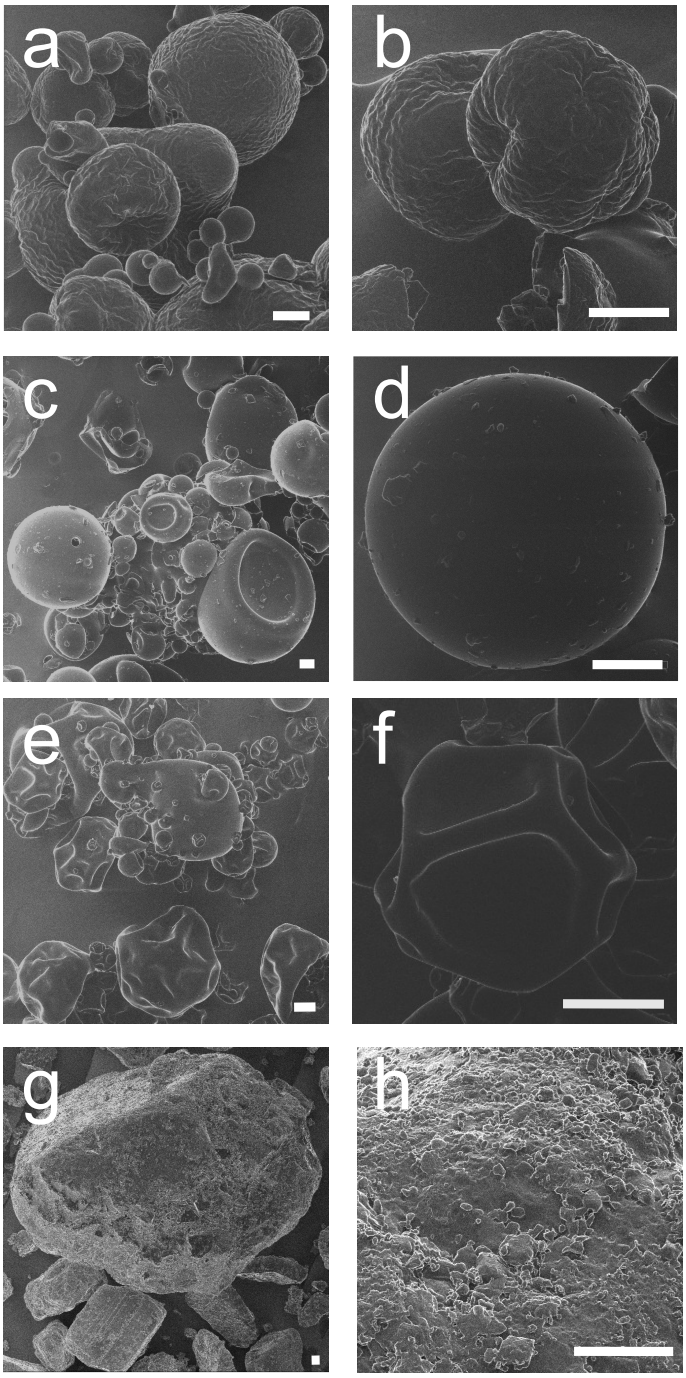

Figure 1: Scanning helium ion microscopy images of dairy derived powders. Skim milk powder (a-b). Whey protein isolate (c-d). Micellar Casein Isolate (e-f). Lactose powder (g-h). Scale bar 10 μm

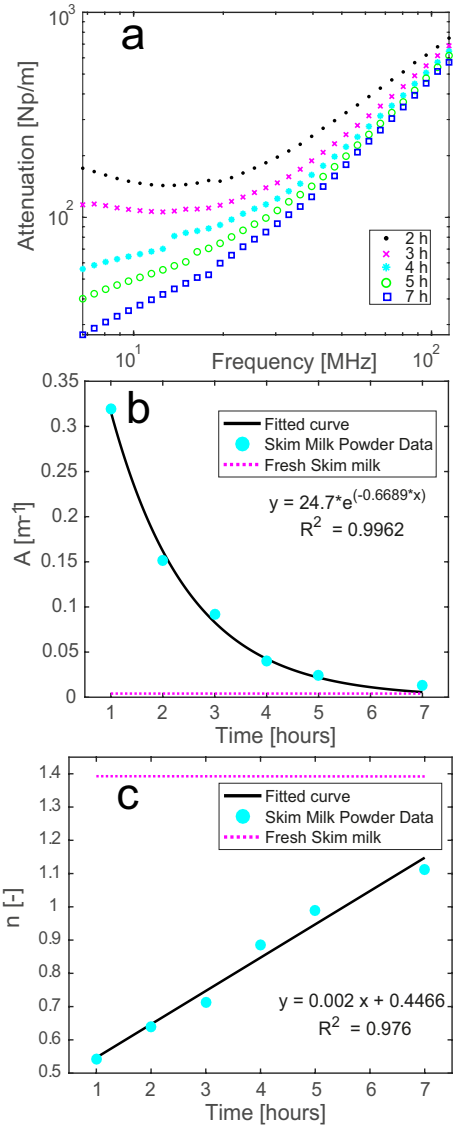

Figure 2: Acoustic monitoring of a skim milk powder dispersion over time. Acoustic Attenuation Spectra of the hydrating system over time (a). The pre-factor component of the attenuation coefficient over time for hydrating skim milk powder dispersion, with an exponential fit to the data, plotted with the value of fresh skim milk (b). The exponent factor of attenuation over time for hydrating skim milk powder dispersion, with a linear fit to the data, plotted with the value of fresh skim milk (c).

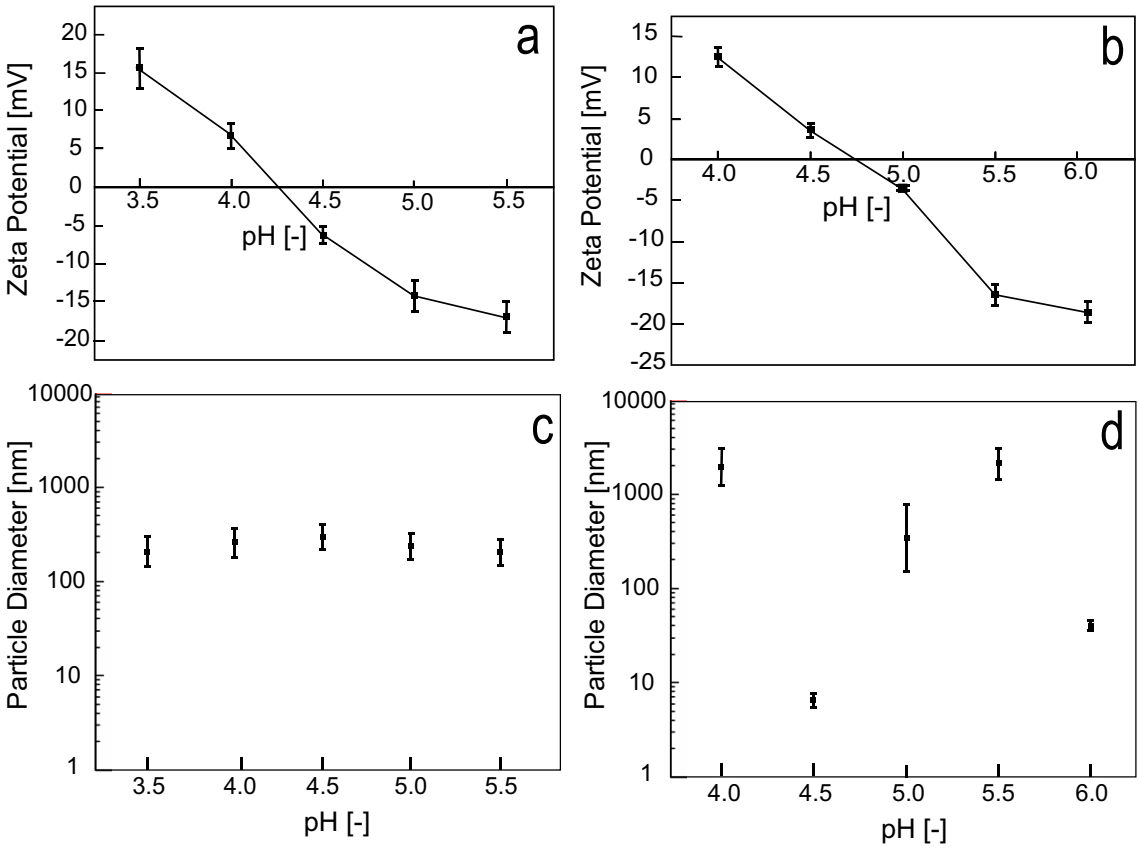

Figure 3: Zeta potential and mean particle size of SMP and WPI dispersions as a function of pH. Zeta potential of SMP dispersion as a function of pH (a). Zeta potential of WPI as a function of pH (b). Mean particle size of SMP dispersion as a function of pH (c). Mean particle size of WPI dispersion as a function of pH (d).

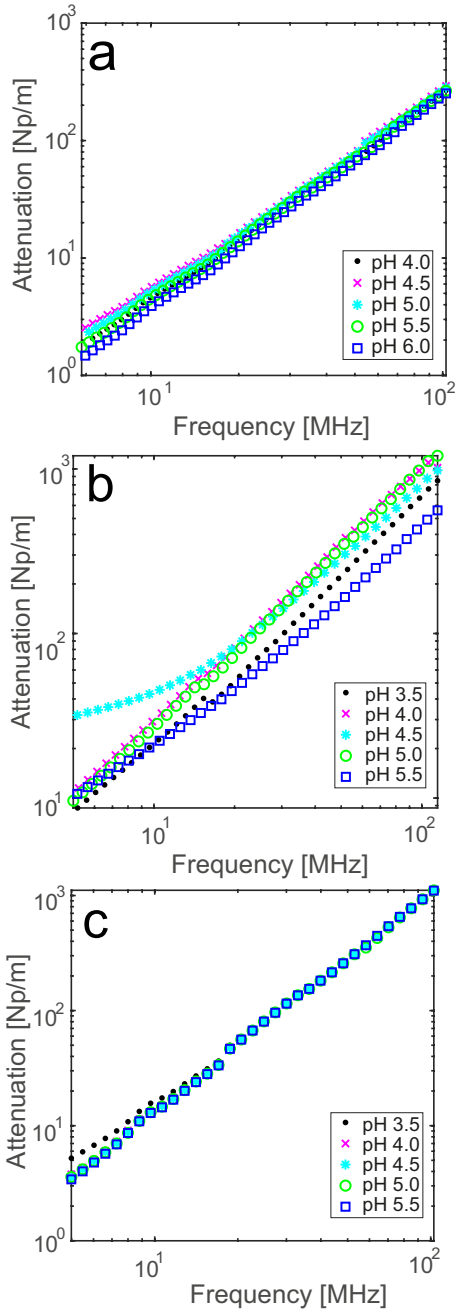

Figure 4: Attenuation spectra of reconstituted dairy systems as a function of pH measured 1 hour after reconstitution. Reconstituted whey protein isolate (a). Reconstituted skim milk powder (b). Reconstituted lactose (c).

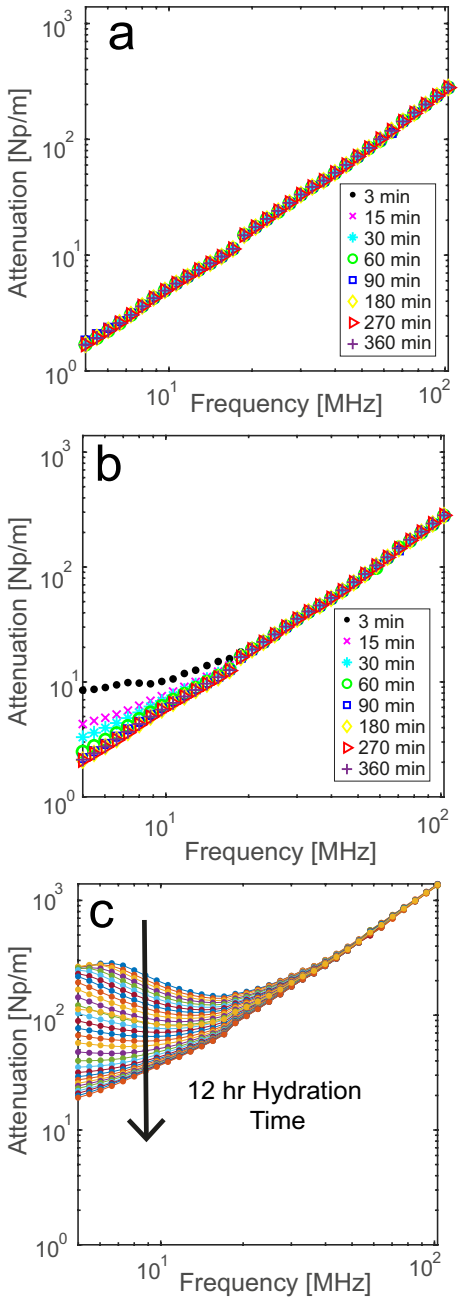

Figure 5: Attenuation spectra for recombined dairy systems over time. Recombined micellar casein isolate and Lactose (a). Recombined micellar casein isolate and whey protein isolate (b). Attenuation spectra for a recombined system of micellar casein isolate, whey protein isolate and lactose, over a 12 hour rehydration time (c).

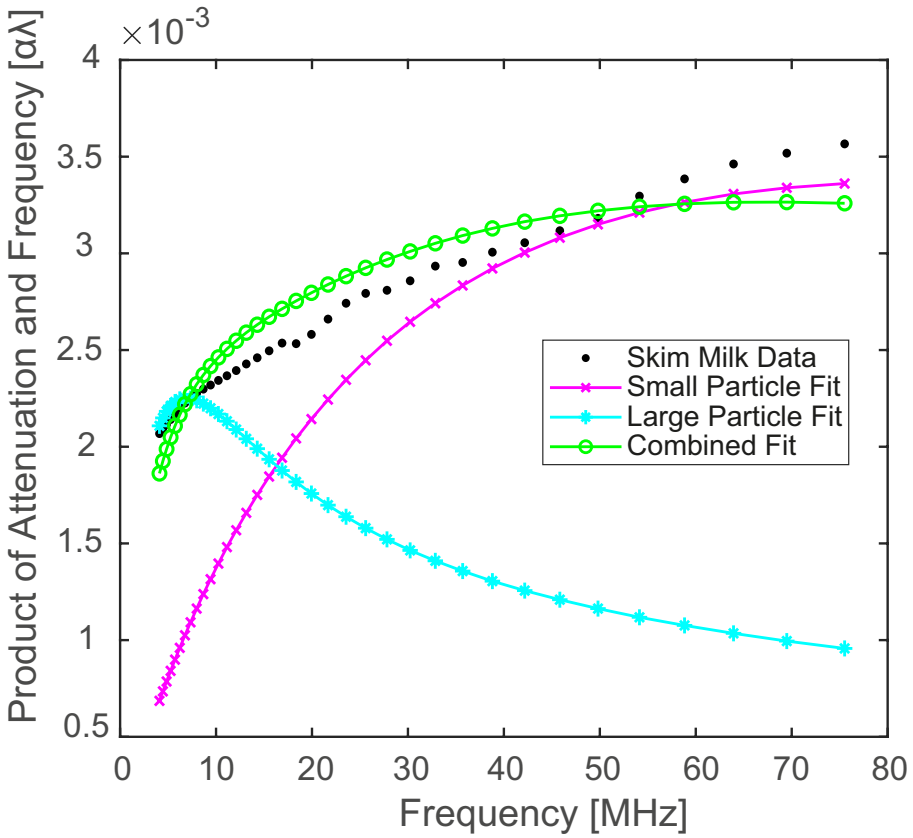

Figure 6: ECAH model fitting to attenuation data of fresh skim milk. Skim milk data plotted in black dots. A large particle fit, to the lower frequency data, is shown with cyan asterisks, and a small particle fit, to the higher frequency data, is shown in magenta crosses. A combined fit is shown in green circles. Volume fractions and particle sizes can be determined from the fitted data for each population.

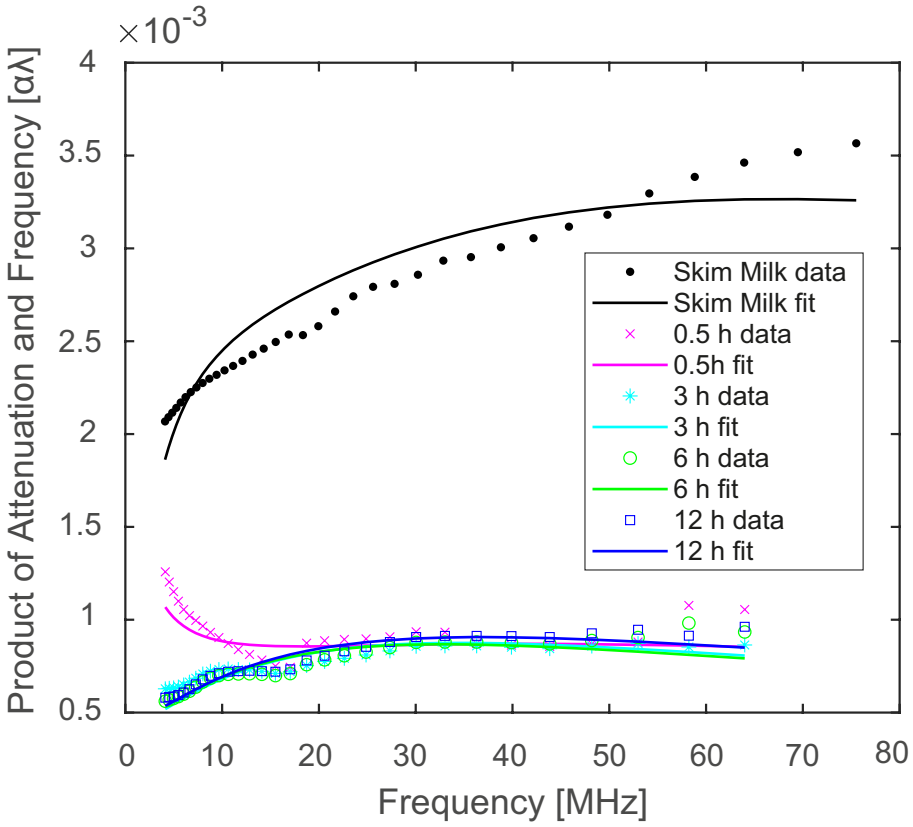

Figure 7: Data inversion for a recombined dairy system compared to fresh skim milk. Attenuation data from fresh skim milk, and recombined system of micellar casein isolate, whey protein isolate and lactose as shown in a, at times 0.5, 3, 6 and 12 hours rehydration. Data is shown with combined small and large particle fits, generated as shown in figure 6.